Neuroradiology (1994) 36: 350–354

Neuro radiology

Assessment of CSF dynamics and venous flow in the superior sagittal sinus by MRI in idiopathic intracranial hypertension: a preliminary study

P. Gideon[1], P. S. Sørensen[2], C. Thomsen[1], F. Ståhlberg[1,3], F. Gjerris[4], O. Henriksen[1]

[1] Danish Research Center of Magnetic Resonance, Hvidovre Hospital, University of Copenhagen, Denmark
[2] Department of Neurology, Rigshospitalet, University of Copenhagen, Denmark
[3] Department of Radiation Physics, Lund University Hospital, Sweden
[4] Department of Neurosurgery, Rigshospitalet, University of Copenhagen, Denmark

Received: 20 June 1993/Accepted: 6 September 1993

Abstract. A velocity-sensitive magnetic resonance imaging (MRI) phase-mapping method was used for noninvasive study of cerebrospinal fluid (CSF) flow in the cerebral aqueduct, for indirect calculation of supratentorial CSF production, and for measurement of blood flow in the superior sagittal sinus (SSS). We examined 12 patients with idiopathic intracranial hypertension (IIH; pseudotumour cerebri), and 10 healthy volunteers. The peak caudal and rostal CSF flow in the aqueduct during the cardiac cycle did not differ significantly between the patients and the volunteers. A significant correlation was found between the CSF volume flow amplitude and the resistance to cerebrospinal fluid outflow in the patients ($p < 0.05$). The calculated mean supratentorial CSF production rate was 0.79 ml/min in the patients and 0.70 ml/min in the controls, but this difference was not statistically significant. However, the MRI measurements suggested CSF hypersecretion in three patients, whereas increased transependymal passage of CSF could have been the cause of negative calculated CSF production rates in two others. A tendency towards lower mean blood flow in the SSS (mean 345 ml/min) in the patients than in the controls (mean 457 ml/min) was found, and in two patients showed very low values. We showed that MRI phase-mapping may be used to study the relative importance of the pathophysiological factors thought to play a role in the development of IIH.

Key words: MRI – CSF flow – CSF production – Blood flow, superior sagittal sinus – Pseudotumour cerebri – Benign intracranial hypertension

Idiopathic intracranial hypertension (IIH), also known as benign intracranial hypertension or pseudotumour cerebri, is characterised by increased intracranial pressure (ICP) in the absence of an intracranial space-occupying lesion. Standard magnetic resonance imaging (MRI) and computed tomography reveal no abnormality and the size of the ventricular system is normal. The cerebrospinal fluid (CSF) is normal [1–4]. The incidence of IIH is approximately 0.9 per 100,000 persons, and in obese women of childbearing age as high as 19 per 100,000 persons [1, 3, 4]. IIH is often a chronic disorder, and can lead to severe visual loss or blindness [2, 4, 5]. IIH is probably not a single clinical entity, and its pathogenesis may vary in different patients. Pathophysiological mechanisms suggested as the cause include increased brain volume caused by increased water content [6, 7], increased blood volume [7, 8], increased rate of CSF formation [9, 10], and decreased rate of CSF absorption at the arachnoid villi [2, 11–14]. Thrombosis of the superior sagittal sinus (SSS) can produce the picture of IIH.

MRI velocity-mapping methods permit noninvasive studies of the to-and-fro motion of CSF in the cerebral aqueduct and indirect measurement of both supratentorial CSF production and flow in major blood vessels [15–21]. Our purpose was to assess the diagnostic value of measurements of CSF velocity and volume flow in the cerebral aqueduct, supratentorial CSF production and blood flow in the SSS in patients with IIH, using a MRI velocity-mapping method.

Materials and methods

We examined 12 patients (8 women and 4 men) with IIH; the age range was 12–61 years (mean ± SD, 37.6 ± 15.4 years) (Table 1). The diagnostic criteria for IIH were: (1) Increased ICP (steady state ICP > 15 mm Hg). (2) Symptoms and signs of increased ICP, without any localising signs, other than a sixth nerve palsy. (3) No focal or diffuse pathology on MRI. (4) Normal or low protein concentration and normal cell count in the CSF. (5) No clinical or neuroradiological suspicion of venous sinus thrombosis. Patients who were taking medication such as furosemide and acetazolamide to reduce CSF production discontinued the treatment at least 72 h prior to the MRI examination. ICP was monitored via a lumbar cannula, and the resistance to CSF outflow (R_{out}) was measured by a lumbar infusion test [13, 14]. The R_{out} is the reciprocal value of the

Correspondence to: P. Gideon, Danish Research Center of Magnetic Resonance, Hvidovre Hospital, Kettegaard allé 30, DK-2650 Hvidovre, Denmark

Table 1. Patients with idiopathic intracranial hypertension (IIH)

Patient	Age/sex (years)	Duration of symptoms (months)	Mean ICP[a] (mm Hg)	R_{out}[b] (mm Hg/ml/min)
1	12/M	2	22	9.4
2	24/F	1	50	23.9
3	26/M	4	28	11.5
4	42/F	36	18	14.8
5	32/F	24	18	15.0
6	46/F	30	26	9.1
7	34/M	1	27	37.2
8	19/F	1	26	7.3
9	51/F	28	28	14.2
10	52/F	78	20	8.3
11	52/M	1	30	22.6
12	61/F	29	25	37.2

[a] *ICP* intracranial pressure (normal value < 15 mm Hg) [b] R_{out} resistance to CSF outflow (normal value < 9.10 mm Hg/ml/min)

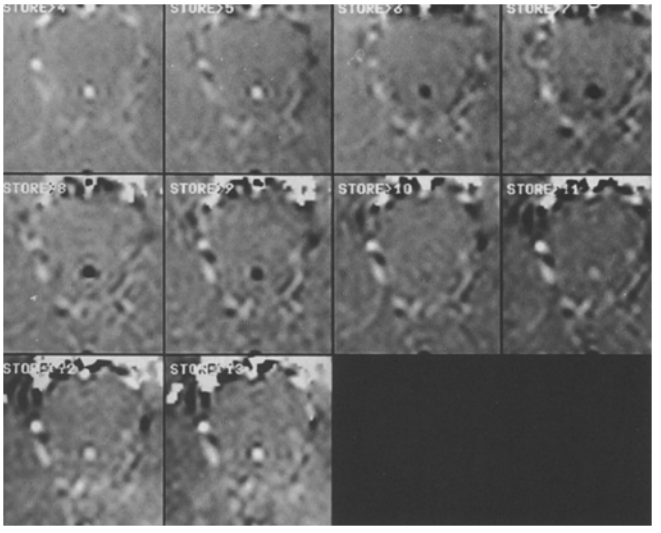

Fig. 1. Ten phase maps, showing the cerebral aqueduct, equally spaced within the cardiac cycle in one patient. High phase signal signifies rostral flow and low signal caudal flow

conductance to CSF outflow [13, 14, 22], and is 9.10 mm Hg/ml/min or less in healthy volunteers [22].

Ten healthy volunteers (4 women and 6 men) aged 22–63 years (mean ± SD, 35.9 ± 14.6 years), with no history of neurological disease, served as controls. The study was approved by the Ethics Committee for Copenhagen and Frederiksberg municipalities, and informed consent was obtained in all cases.

An MR imager operating at 1.5 Tesla, with a standard head coil was used. The brain was imaged with a standard double spin-echo (SE) sequence in the axial plane, with repetition time (TR) 2.2 s, and echo times (TE) 15 and 90 ms, and T1-weighted SE images with TR 0.5 s and TE 15 ms in axial and sagittal planes. Slice thickness was 6 mm with an interslice distance of 6 mm; subsequently the interslice spaces were imaged using the same sequence. The field of view was 300 mm, and matrix size 256 × 256.

For velocity-mapping of aqueductal CSF, the subjects were placed supine. The head was carefully extended approximately 20 degrees in order to place a slice in the axial plane exactly perpendicular to the cerebral aqueduct at the level of the inferior colliculi; fixation was obtained using a deflatable pillow. Slice thickness was 8 mm, field of view 215 cm and matrix size 256 × 128 interpolated to 256 × 256, giving a voxel size of 0.84 × 0.84 × 8 mm^3. As CSF pulsates to-and-fro in the aqueduct with the pulse, ECG triggering was used [15–21, 23]. All examinations were carried out within a 4 h period in the afternoon, to avoid the effects of circadian variations in CSF production [20]. CSF movement (hereafter referred to as flow) in the aqueduct was examined using two specially designed fast low-angle shot (FLASH) sequences, with echo time 15 ms and a flip angle 30° [16, 17], executed in an interleaved mode to give velocity sensitivity. With both sequences, three gradient lobes were used in the slice-select direction, which was also the flow-sensitive direction. The first sequence was velocity-compensated while the second sequence was sensitive to slowly flowing CSF. To cover the full R-R interval, each train of coded or noncoded pulse sequences was executed during 100 % of the R-R interval, triggering on every second R wave. Thus the noncoded pulse sequence train was triggered on the first R wave, covering the full R-R interval, while the coded pulse sequence train was triggered on the third R wave covering the full R-R interval. The TR was set to one tenth of the R-R interval, giving 10 + 10 phase images covering the entire cardiac cycle in 2 × 256 heart beats, or between 6–12 min depending upon heart rate. After subtraction of the corresponding phase images obtained with the two sequences, ten phase maps equally distributed over the entire cardiac cycle were obtained (Fig. 1). To calculate the average CSF velocity in the aqueduct, the phase signal within it was determined by placing a circular region of interest (ROI), whose area ranged between 11–15 mm^3, corresponding to 16–21 pixels, over it. Additional ROI were placed on both sides of the aqueduct, within the stationary mesencephalon, to determine the phase background; to correct for phase offset, the phase background was subtracted from the phase signal in the aqueduct [17]. The phase signal was proportional to velocity [17], and the velocity corresponding to a phase angle of π was 137 mm/s. Phase noise on our system was approximately +/– 2 mm/s [17]. Volume flow was obtained by multiplying the average CSF velocity by the area of the aqueduct [15, 17]. The linear velocity will be underestimated if the ROI is larger than the cerebral aqueduct and overestimated if it is smaller, whereas estimation of volume flow is less sensitive, provided the ROI is as least as large the aqueduct, because overestimation of the average velocity is compensated for by overestimation of the cross-sectional area [24]. Supratentorial CSF production was calculated in ml/min, as the difference between net CSF inflow and net CSF outflow over the cardiac cycle [17]. There is a cumulative error of approximately 30 % in the calculation of CSF production using this indirect method, partly due to fluctuations in the length of the R-R interval caused by breathing [16, 17]. CSF flow measurements were executed twice, without repositioning, in all subjects, and the mean values were used.

Blood flow in the SSS was measured using a similar interleaved FLASH sequence, in which the velocity corresponding to a phase angle of π was 1046 mm/s. The measurement was performed on the same slice as the CSF measurements, approximately 4 cm above the torcular. An ROI was drawn over the SSS, its ROI ranging from 11 to 73 mm^3, or 16–103 pixels, and additional circular ROI were placed on both sides of the SSS, to correct for phase offset.

The parameters of CSF flow in the aqueduct we studied were: peak velocity and volume flow in caudal and rostral directions and the time to peak caudal flow expressed as a percentage of the length of the cardiac cycle. Supratentorial CSF production in ml/min and mean SSS blood flow in ml/min were also calculated.

The Mann-Whitney rank sum test for unpaired samples was used to compare the results. The level of significance was set at $p < 0.05$.

Results

Of the 12 IIH patients 11 had headache, 7 had visual obscurations, 2 blurred vision, 4 diplopia, and 3 had sixth nerve palsies, one bilateral and 2 on the left. The duration of symptoms was 1–78 months. Six of the female patients were more than 25 % overweight, and one patient was

Table 2. CSF flow in the cerebral aqueduct, supratentorial CSF production and blood flow in the superior sagittal sinus (SSS) in patients with IIH

Patient	Peak CSF flow (ml/min)		CSF production (ml/min)	Blood flow in SSS (ml/min)
	caudal	rostral		
1	3.3	3.3	0.81	–
2	2.6	5.2	–0.79	491
3	5.9	2.8	1.74	270
4	12.6	7.6	1.37	83
5	6.8	5.1	0.71	354
6	4.9	4.9	0.17	386
7	11.4	5.1	3.47	314
8	1.9	0.8	0.41	443
9	3.1	1.9	0.35	–
10	5.5	2.3	0.64	741
11	7.8	8.2	–0.26	41
12	11.3	6.5	0.85	327
Mean	6.4	4.5	0.79	345
SD	3.7	2.3	1.08	199

Table 3. CSF flow in the cerebral aqueduct, supratentorial CSF production and blood flow in the superior sagittal sinus (SSS) in ten healthy volunteers

Subject	Peak CSF flow (ml/min)		CSF production (ml/min)	Blood flow in SSS (ml/min)
	caudal	rostral		
1	4.3	1.8	0.87	592
2	3.2	2.5	0.83	505
3	5.5	3.3	0.34	316
4	9.5	7.0	1.22	523
5	3.8	1.9	0.60	481
6	1.3	0.9	0.22	305
7	4.0	1.6	0.92	673
8	2.9	3.0	0.34	333
9	4.6	2.6	0.77	541
10	4.1	3.7	0.85	300
Mean	4.3	2.8	0.70	457
SD	2.1	1.7	0.31	134

Table 4. Findings in two patients examined serially

Patient	Timing of study	Peak CSF flow (ml/min)		CSF production (ml/min)	Blood flow in SSS (ml/min)
		Caudal	Rostral		
2	1 month	2.6	5.2	–0.79	491
	5 months	2.0	2.7	–0.24	577
	9 months	4.1	4.1	–0.22	493
8	1 month	1.9	0.8	0.41	443
	5 months	2.3	2.0	0.24	469

taking oxcarbazepine, which may provoke intracerebral water accumulation; four patients had received treatment with furosemide and acetazolamide. MRI of the brain was normal in all 12. At the time of the MRI examination the average ICP of the patients was 26.5 mm Hg; 9 had increased values of R_{out} (Table 1), and 2 had constant B-wave activity during ICP monitoring.

The CSF peak volume flow in the aqueduct, supratentorial CSF production, and mean flow in the SSS are shown in Tables 2 and 3. The CSF flow curve, within the R-R interval, was basically sinosoidal in both patients and controls. In the patients, the peak velocities ranged

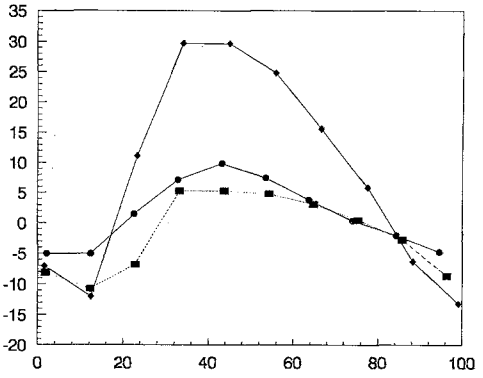

Fig. 2. CSF flow velocity curves from the cerebral aqueduct through one cardiac cycle in patient 2 (■), patient 7 (◆) and one healthy volunteer (●). The x-axis is the percentage of the cardiac cycle, and the y-axis CSF flow velocity (mm/s)

from 4.9 to 32.9 mm/s caudal and from 2.0 to 19.8 mm/s rostrally. The corresponding values for the controls were 3.4–24.7 mm/s and 2.2–18.3 mm/s; there was no significant difference in the peak velocity or volume flow in either direction between patients and controls. The correlation coefficient between the total CSF volume flow amplitude and R_{out} was $r = 0.66$ ($p < 0.05$). The peak caudal flow was reached after 42 % of the cardiac cycle in the controls and after 44 % in the patients.

The mean supratentorial CSF production was 0.70 ml/min (range 0.22–1.22 ml/min) in the controls and 0.79 ml/min (range –0.79–3.47 ml/min) in the patients; this difference was not statistically significant. There was relatively large standard deviation in the calculated values in the patients, 3 had CSF hypersecretion, defined as production exceeding the mean value of the controls plus two standard deviations. In two patients negative production values were calculated; in one of these, negative production values were found at three separate examinations. The CSF velocity flow curves within a cardiac cycle of a healthy volunteer and two patients 2 and 7 are shown in Fig. 2.

Mean blood flow in the SSS was 457 ml/min (range 300–673 ml/min) in the controls and 345 ml/min in the patients; this was not statistically significant (Table 3). Two patients had very low mean blood flow values of 41 and 83 ml/min, but had no signs of SSS thrombosis on conventional MRI.

We reexamined two patients (Table 4). Patient 2 was studied 4 months after the initial examination, because of continuing symptoms in spite of treatment with furosemide and acetazolamide; her ICP was 40 mm Hg at this time. She was studied again 8 months after the initial examination, following a ventriculoperitoneal shunt operation. Patient 8 was examined four months after the initial study. She received no treatment, and her symptoms were resolving. No major changes with time in the calculated peak CSF volume flow, CSF production or blood flow in the SSS were found in these patients. Patient 2 continued to have apparently negative supratentorial CSF production.

Discussion

The CSF velocities and volume flow measured in the aqueduct in this study demonstrate that a substantial variation exists in healthy individuals. Partial volume effects are unavoidable in the determination of CSF flow within the aqueduct, due in part to the size of the aqueduct relative to that of the voxel, and in part to the relatively thick slices. The results are in good agreement with those from previous velocity-mapping studies [17–21]. Quencer et al. [18] found caudal CSF velocities in the aqueduct ranging from 3.7 to 7.6 mm/s, and Enzmann and Pelc [19] mean peak caudal and rostral velocities of 11.8 and 11.6 mm/s, respectively, in healthy volunteers. Increased peak flow velocity and peak volume flow have been demonstrated in patients with normal pressure hydrocephalus [21, 25]. Our values for CSF velocities and volume flow, in the patients with IIH, demonstrated considerable variation. In some patients the values were outside the range of the healthy controls, possibly reflecting different pathophysiological mechanisms responsible for the increased ICP.

A statistically significant correlation was found between the total CSF volume flow amplitude, and R_{out} in the patients. As an increased R_{out} signifies decreased compliance of the brain tissue, this finding seems reasonable. Fourier analysis of the CSF velocity flow curves [17], showed no apparent difference between patients and controls. Peak caudal flow occurred after 42 % (mean value) of the cardiac cycle in healthy volunteers, after 44 % in patients with IIH, and in a similar study of patients with normal pressure hydrocephalus [25], after 45 %.

Mean supratentorial CSF production in controls was 0.70 ml/min, or i.e., almost 1 litre/24 h; this is in agreement with previous studies using this technique [17, 20, 25]. Feinberg and Mark [15] calculated a rate of 0.47 ml/min in one healthy volunteer, while and Enzmann and Pelc [23] found a mean rate of 0.34 ml/min in 10 healthy volunteers. In a recent study Nilsson et al. [20] found a circadian variation in human CSF production using the present method, production being slowest around noon, and most rapid around midnight [20]. This suggests that it is necessary to perform the measurements within a narrow time limit to obtain a meaningful comparison. Our measurements were all performed within a 4 h period in the late afternoon; the values we obtained therefore presumably represent an intermediate production rate. Since CSF production from the ventricular system rostral to the aqueduct may account for only 60–70 % of the total [26], total CSF production will be underestimated. In previous studies using ventriculolumbar perfusion, the average CSF production rate, in humans with malignant disease, was approximately 0.35 ml/min [27, 28]. May et al. [29] in a recent study of healthy volunteers, using a modified Masserman method, found mean production rates of 0.41 ml/min in the young and 0.19 ml/min in the elderly [29]. The production rates calculated from noninvasive MR velocity-mapping methods therefore seem somewhat higher than suggested by previous invasive studies. In patients with normal pressure hydrocephalus, we found a mean production rate of 0.60 ml/min [25]. Donaldson [9, 10] suggested CSF hypersecretion as an explanation for increased ICP in obese young women with IIH. Our results do not support the suggestion that hypersecretion is an important factor in the majority of patients with IIH. In some, however, increased CSF production may contribute to the development of intracranial hypertension. If CSF hypersecretion alone were to be responsible for the increased ICP, one would probably have to assume that the production rate was increased by a factor of at least three or four [10]. A production rate of this magnitude was found in only one of our patients, suggesting that in this patient CSF hypersecretion could perhaps be the cause of the increased ICP. In patients 3 and 4 a relatively high production rate was also found. Malm et al. [30], using a constant-pressure infusion method, found no difference in CSF production between patients with IIH and healthy volunteers. The cumulative error in calculation of the CSF production rate was approximately 30 % [17], and this could explain the negative production rates found in two of our patients. However, as repeated examinations of one of them all gave negative production values (Table 4), this could perhaps be taken as evidence of increased transependymal CSF resorption.

Our mean value of 457 ml/min for blood flow in the SSS in healthy volunteers, is in good agreement with the results of Mattle et al. [31], who found a mean flow of 420 ml/min, using a bolus-tracking MRI method. There was a tendency towards lower blood flow in the patients, but this was not statistically significant. Two patients showed marked reduction of the blood flow. One might speculate that these patients might have had an otherwise subclinical thrombosis of the SSS as the cause of IIH. As no evidence of permanent thrombosis was seen at conventional MRI, partial recanalisation may have occured, but we have no evidence that this is the case. In future studies of IIH it might be advisable to perform MR angiography to elucidate this possibility.

Acknowledgements. This study was supported by the Danish Health Research Council, grant no. 12-96356. The Scandinavian Flow Group is acknowledged for its support.

References

1. Durcan FJ, Corbett JJ, Wall M (1988) The incidence of pseudotumour cerebri. Population studies in Iowa and Louisiana. Arch Neurol 45: 875–877
2. Sørensen PS, Krogsaa B, Gjerris F (1988) Clinical course and prognosis of pseudotumour cerebri. A prospective study of 24 patients. Acta Neurol Scand 77: 164–177
3. Giuseffi V, Wall M, Siegel P, Rojas PB (1991) Symptoms and disease associations in idiopathic intracranial hypertension (pseudotumour cerebri): a case-control study. Neurology 41: 239–244
4. Wall M, George D (1991) Idiopathic intracranial hypertension. A prospective study of 50 patients. Brain 114: 155–180
5. Corbett JJ, Savino PJ, Thompson HS, Kansu T, Schatz NJ, Orr LS, Hopson D (1982) Visual loss in pseudotumour cerebri. Follow-up of 57 patients from five to 41 years and a profile of 14 patients with permanent severe visual loss. Arch Neurol 39: 461–474

6. Raichle ME, Grubb RL, Phelps ME, Gado MH, Caronna JJ (1978) Cerebral hemodynamics and metabolism in pseudotumour cerebri. Ann Neurol 4: 104–111
7. Sørensen PS, Thomsen C, Gjerris F, Schmidt J, Kjær L, Henriksen O (1989) Increased brain water content in pseudotumour cerebri measured by magnetic resonance imaging of brain water self diffusion. Neurol Res 11: 160–164
8. Dandy WE (1937) Intracranial pressure without brain tumour. Ann Surg 106: 492–513
9. Donaldson JO (1979) Cerebral fluid hypersecretion in pseudotumour cerebri. Trans Am Neurol Assoc 104: 196–198
10. Donaldson JO (1981) Pathogenesis of pseudotumour cerebri syndromes. Neurology 31: 877–880
11. Johnston I, Paterson A (1974) Benign intracranial hypertension. II. CSF pressure and circulation. Brain 97: 301–312
12. Sklar FH, Beyer CW, Ramanathan M, Cooper PR, Kemp Clark W (1979) Cerebrospinal fluid dynamics in patients with pseudotumour cerebri. Neurosurgery 5: 208–216
13. Gjerris F, Sørensen PS, Vorstrup S, Paulson OB (1985) Intracranial pressure, conductance to cerebrospinal fluid outflow, and cerebral blood flow in patients with benign intracranial hypertension (pseudotumour cerebri). Ann Neurol 17: 158–162
14. Gjerris F, Børgesen SE (1992) Current concepts of measurement of cerebrospinal fluid absorption and biomechanics of hydrocephalus. In: Symon L et al. (eds) Advances and technical standards in neurosurgery, vol 19. Springer, Wien, New York, pp 145–177
15. Feinberg DA, Mark AS (1987) Human brain motion and cerebrospinal fluid circulation demonstrated with MR velocity imaging. Radiology 163: 793–799
16. Ståhlberg F, Møgelvang J, Thomsen C, Nordell B, Stubgaard M, Ericsson A, Sperber G, Greitz D, Larsson H, Henriksen O, Persson B (1989) A method for quantification of flow velocities in blood and CSF using interleaved gradient-echo pulse sequences. Magn Res Imag 7: 655–667
17. Thomsen C, Ståhlberg F, Stubgaard M, Nordell B, The Scandinavian Flow Group (1990) Fourier analysis of cerebrospinal fluid flow velocities: MR imaging study. Radiology 177: 659–665
18. Quencer RM, Post MJD, Hinks RS (1990) Cine MR in the evaluation of normal and abnormal CSF flow: intracranial and intraspinal studies. Neuroradiology 32: 371–391
19. Enzmann DR, Pelc NJ (1991) Normal flow patterns of intracranial and spinal cerebrospinal fluid defined with phase-contrast cine MR imaging. Radiology 178: 467–474
20. Nilsson C, Ståhlberg F, Thomsen C, Henriksen O, Herning M, Owman C (1992) Circadian variation in human cerebrospinal fluid production measured by magnetic resonance imaging. Am J Physiol 262: R20–R24
21. Nitz WR, Bradley WG, Watanabe AS, Lee RR, Burgoyne B, O'Sullivan RM, Herbst MD (1992) Flow dynamics of cerebrospinal fluid: assessment with phase-contrast velocity MR imaging performed with retrospective cardiac gating. Radiology 183: 395–405
22. Albeck MJ, Børgesen SE, Gjerris F, Schmidt JF, Sørensen PS (1991) Intracranial pressure and cerebrospinal fluid outflow conductance in healthy subjects. J Neurosurg 74: 597–600
23. Enzmann DR, Pelc NJ (1992) Brain motion: measurement with phase-contrast MR imaging. Radiology 185: 653–660
24. Thomsen C, Ståhlberg F, Henriksen O (1993) Quantification of portal venous blood flow during fasting and after a standardized meal – a MRI phase-mapping study. Eur Radiol 3: 242–247
25. Gideon P, Ståhlberg F, Thomsen C, Gjerris F, Sørensen PS, Henriksen O (1994) Cerebrospinal fluid flow and production in patients with normal pressure hydrocephalus studied by MRI. Neuroradiology 36: 210–215
26. Davson H, Welch K, Segal MB (1987) The physiology and pathophysiology of the cerebrospinal fluid. Churchill Livingstone, Edinburgh, pp 189–203
27. Rubin RC, Henderson ES, Ommaya AK, Walker MD, Rall DP (1966) The production of cerebrospinal fluid in man and its modification by acetazolamide. J Neurosurg 25: 430–436
28. Cutler RWP, Page L, Galicich J, Watters GV (1968) Formation and absorption of cerebrospinal fluid in man. Brain 91: 707–720
29. May C, Kaye JA, Atack JR, Schapiro MB, Friedland RP, Rapoport SI (1990) Cerebrospinal fluid production is reduced in healthy aging. Neurology 40: 500–503
30. Malm J, Kristensen B, Markgren P, Ekstedt J (1992) CSF hydrodynamics in idiopathic intracranial hypertension: a long term study. Neurology 42: 851–858
31. Mattle H, Edelman RR, Reis MA, Atkinson DJ (1990) Flow quantification in the superior sagittal sinus using magnetic resonance. Neurology 40: 813–815